TECHNOMETRICS
2017, VOL. 0, NO. 0, 1–13
https://doi.org/10.1080/00401706.2017.1321584

Taylor & Francis
Taylor & Francis Group

Semiparametric Models for Accelerated Destructive Degradation Test Data Analysis

Yimeng Xie[a], Caleb B. King[a], Yili Hong[a], and Qingyu Yang[b]

[a]Department of Statistics, Virginia Tech, Blacksburg, VA; [b]Department of Industrial and Systems Engineering, Wayne State University, Detroit, MI

ABSTRACT

Accelerated destructive degradation tests (ADDT) are widely used in industry to evaluate materials' long-term properties. Even though there has been tremendous statistical research in nonparametric methods, the current industrial practice is still to use application-specific parametric models to describe ADDT data. The challenge of using a nonparametric approach comes from the need to retain the physical meaning of degradation mechanisms and also perform extrapolation for predictions at the use condition. Motivated by this challenge, we propose a semiparametric model to describe ADDT data. We use monotonic B-splines to model the degradation path, which not only provides flexible models with few assumptions, but also retains the physical meaning of degradation mechanisms (e.g., the degradation path is monotonic). Parametric models, such as the Arrhenius model, are used for modeling the relationship between the degradation and the accelerating variable, allowing for extrapolation to the use condition. We develop an efficient procedure to estimate model parameters. We also use simulations to validate the developed procedures and demonstrate the robustness of the semiparametric model under model misspecification. Finally, the proposed method is illustrated by multiple industrial applications. This article has online supplementary materials.

ARTICLE HISTORY
Received December 2015
Revised March 2017

KEYWORDS
Acceleration model; ADDT; Arrhenius model; Degradation model; Long-term property evaluation; Polymeric materials

1. Introduction

1.1 Motivation

It is important for manufacturers to understand the lifetime of their products to ensure accurate marketing and determine areas for improvement. While lifetime testing is the most common approach, for many materials it is more informative to observe the degradation of some performance characteristics over time, such as the tensile strength of an adhesive bond. The lifetime is determined by a "soft failure" when the characteristic crosses a predetermined level. This form of testing is known as degradation testing.

Several varieties of degradation testing have been developed to accommodate unique circumstances. Due to the long service life of many new materials, degradation testing under a normal use condition is often not feasible. By exposing the material to a more harsh environment, such as higher levels of temperature or humidity compared to the use condition, degradation data can be collected more efficiently. Thus, an accelerating variable is often used in degradation tests. In some applications, measurements of the degradation level are destructive. That is, the units being tested are destroyed or the physical characteristics changed in a significant manner. Because the test is destructive, only one measurement can be taken from one unit. An example could be determining the strength of a material by measuring the force needed to break it. This form of testing, combined with an accelerating variable, is referred to as accelerated destructive degradation testing (ADDT). To differentiate, another common form of degradation testing is repeated-measures degradation testing (RMDT), in which the measurement is nondestructive and multiple measurements can be taken from the same unit. Because of the nature of the testing, ADDT must be analyzed differently from RMDT. The objectives of the inference are often different. For example, the focus of the inference from ADDT data is primarily on the population behavior (e.g., population quantiles, mean time to failure), while for RMDT data the inference can be done at individual unit level (e.g., the distribution of remaining life for a particular unit). The focus of this article, however, is on the modeling and analysis of ADDT data.

ADDT is commonly used in industrial practice, for example, to evaluate the long-term properties for polymeric materials. In this article, we use the adhesive bond B data (Escobar et al. 2003), the seal strength data (Li and Doganaksoy 2014), and the adhesive formulation K data for illustrations. The details of these examples are presented in Section 5. In the literature, the analyses of those ADDT datasets involved assumed parametric models for the degradation path over time and a parametric form for the accelerating-variable effect. The predominance of parametric models is mainly due to the need for extrapolation in two aspects; extrapolation in time and extrapolation to the use condition. For example, an ADDT may cover only a 30% reduction of the material's original strength at an elevated temperature range (e.g., 60°C–80°C). But interest lies at 50% reduction of the original strength at a use temperature (e.g., 30°C). Despite their usefulness in extrapolation, the major

CONTACT Yili Hong yilihong@vt.edu
Color versions of one or more of the figures in the article can be found online at www.tandfonline.com/r/TECH.
Supplementary materials for this article are available online. Please go to http://www.tandfonline.com/r/TECH.

limitation of parametric models is that each model is application specific. Thus, it is challenging for an industrial standard, such as UL746B (2013), to recommend a generic method for ADDT data analysis. Another limitation is on the consequence of model misspecification (i.e., the assumed parametric model departs from the true model for the degradation path). A larger mean squared error (MSE) for the parameter estimator could result if a parametric model is misspecified.

On another side, there has been tremendous statistical research in nonparametric methods, although the current industrial practice is still to use application-specific parametric models to describe ADDT data. In this article, we aim to bridge this gap between the statistical research and current industrial practice. Instead of a case-by-case parametric modeling approach, we propose a general and flexible semiparametric model to describe ADDT data, which is new to the ADDT data analysis literature. The challenge of using a nonparametric approach comes from the need to retain the physical meaning of degradation mechanisms and from performing extrapolations for predictions at the use condition. To overcome those challenges, the semiparametric model consists of a nonparametric model for the degradation path and a parametric form for the accelerating-variable effect. To preserve the monotonic nature of many degradation paths, the nonparametric model portion will be constructed based on monotonic spline methods. For the parametric model portion, commonly used models, such as the Arrhenius relationship for temperature, will be used for extrapolation. Parameter estimation and inference procedures will also be developed. Through application demonstration and simulations, we show that the proposed semiparametric model is more flexible, applicable to a wide range of applications, and is more robust to model misspecification. An R package "ADDT" (Hong et al. 2016) is also developed, and the use of the R package is illustrated in Jin et al. (2017). The developed method can be useful for industrial standards, such as UL746B (2013), due to its flexibility and robustness, and software readiness for ADDT data analysis.

1.2 Related Literature

The literature on accelerated degradation data modeling and analysis can be divided into two areas: RMDT and ADDT. In their pioneering work, Lu and Meeker (1993) used RMDT data to estimate a failure-time distribution via a mixed-effects modeling framework. Meeker, Escobar, and Lu (1998) introduced nonlinear mixed-effects models for RMDT data, which were derived from physical-failure mechanisms. An introductory level description of degradation models can be found in Gorjian et al. (2010) and Meeker, Hong, and Escobar (2011). Ye and Xie (2015) provided a comprehensive review of the state-of-art methods in modeling RMDT data.

In the area of ADDT data modeling and analysis, Nelson (1990, chap. 11) used ADDT data to estimate performance degradation. Escobar et al. (2003) provided a parametric model and method to analyze the ADDT data collected from an adhesive bond. Tsai et al. (2013) considered the problem of designing an ADDT with a nonlinear model motivated by a polymer dataset. Li and Doganaksoy (2014) used a parametric model to model ADDT data collected from a temperature accelerated test to study the degradation of seal strength. In all existing methods for analyzing ADDT data, the parametric method is the most popular.

Compared to parametric models of degradation data, spline methods tend to be more flexible and require less assumptions regarding the model formulation. Because the degradation path is often monotonic in nature, monotonic splines are suitable for modeling degradation paths. Ramsay (1988) suggested using a basis of I-splines (integrated splines) for semiparametric modeling. He and Shi (1998) considered the use of B-splines with L_1 optimization. Meyer (2008) extended the work in Ramsay (1988) by proposing cubic monotonic splines. Leitenstorfer and Tutz (2007) considered the use of monotonic B-splines in generalized additive models. For other applications of monotonic B-splines, one can refer to Kanungo, Gay, and Haralick (1995) and Fengler and Hin (2014). In addition, Eilers and Marx (1996) proposed a class of P-splines. Bollaerts, Eilers, and Mechelen (2006), Hofner, Müller, and Hothorn (2011), and Hofner, Kneib, and Hothorn (2016) considered the estimation of monotonic effects with P-splines. We used monotonic B-splines in this article because it provides a wider range of flexibility.

Related to RMDT models, Shiau and Lin (1999) used kernel methods to smooth the average degradation path. The smoothing was done separately for data from each temperature level. Their methods work out well for RMDT data but for ADDT data it is more challenging because the number of time points for each temperature is small, making it hard to smooth over the time horizon. In addition, their method cannot guarantee monotonicity of the underlying degradation path, which could be a problem in ADDT analysis when one needs to extrapolate to the use condition. Zhou, Serban, and Gebraeel (2014) used a spline method to model degradation paths for RMDT data, without considering accelerating variables. Ye et al. (2014)) used a gamma process to model the degradation path with the shape function estimated nonparametrically for RMDT data. Their method also does not have constraints on the degradation paths (i.e., monotonicity) nor does it consider accelerating variables. Other recent developments of stochastic models for RMDT data include Wang and Xu (2010), Ye and Chen (2014), and Peng (2016). However, stochastic models are usually not used for ADDT data because there is only one measure for each test sample. Hong et al. (2015) and Xu, Hong, and Jin (2016) used shape-restricted splines to model the effects of time-varying covariates on the degradation process. There is little literature, however, on the use of semiparametric models in ADDT data modeling and analysis.

1.3 Overview

The rest of this article is organized as follows. Section 2 introduces some general notation for ADDT data. It also presents the construction of the semiparametric model using monotonic B-splines. In Section 3, we present a procedure for estimating the unknown parameters as well as procedures for conducting inference on ADDT data based on the proposed model. We conduct simulation studies in Section 4 to investigate the performance of the semiparametric method with consideration of model misspecification. In Section 5, we apply the model to data from several published datasets and provide comparisons with other well-known parametric models. Finally, Section 6 contains conclusions and areas for future research.

2. The Semiparametric Model

2.1 General Setting

Let y_{ijk} be the degradation measurement for the kth sample at level i of the accelerating variable $\mathcal{AF}_i$ and the jth observation time point t_{ij}, $i = 1, \ldots, n$, $j = 1, \ldots, J_i$, and $k = 1, \ldots, n_{ij}$, where n is the number of accelerating variable levels, J_i is the number of measuring time points for level i, and n_{ij} is the number of samples measured at t_{ij}. Let $N = \sum_{i=1}^{n} \sum_{j=1}^{J_i} n_{ij}$ be the total number of measured samples. A general form of the degradation model is

$$y_{ijk} = \mathcal{D}(t_{ij}, x_i; \boldsymbol{\theta}) + \varepsilon_{ijk}, \tag{1}$$

where $x_i = h(\mathcal{AF}_i)$ is a function of the accelerating variable, $\boldsymbol{\theta}$ is a vector of unknown parameters in the degradation path, and ε_{ijk} is an error term that describes unit-to-unit variability. For the purposes of illustration, we assume that the degradation path is monotone decreasing with time. The model can easily be generalized to paths that are increasing with time. We will also be considering temperature as the accelerating factor as it is the most common form of acceleration encountered in ADDT. However, the model can easily incorporate other types of acceleration, such as voltage.

For temperature-accelerated processes, the Arrhenius model is often used to describe the relationship between the degradation and temperature. This model uses a transformed temperature level, which is given as

$$x_i = h(\mathcal{AF}_i) = \frac{-11605}{\text{Temp}_i + 273.16}. \tag{2}$$

Here, Temp_i is in degrees Celsius, and the value 11,605 is the reciprocal of the Boltzmann's constant (in units of eV). The value 273.16 in the denominator is used to convert to the Kelvin temperature scale.

2.2 The Scale-Acceleration Model

We propose the following semiparametric functional forms for the degradation model in (1).

$$\mathcal{D}(t_{ij}, x_i; \boldsymbol{\theta}) = g[\eta_i(t_{ij}; \beta); \boldsymbol{\gamma}], \tag{3}$$

$$\eta_i(t; \beta) = \frac{t}{\exp(\beta s_i)}, \quad s_i = x_{\max} - x_i, \tag{4}$$

$$\varepsilon_{ijk} \sim \text{N}(0, \sigma^2), \quad \text{and} \quad \text{Corr}(\varepsilon_{ijk}, \varepsilon_{ijk'}) = \rho, \ k \neq k'. \tag{5}$$

Here, $\boldsymbol{\theta} = (\boldsymbol{\gamma}', \beta, \sigma, \rho)'$ is the vector containing all of the unknown parameters. The function $g(\cdot)$ is a monotone decreasing function with unknown parameter vector $\boldsymbol{\gamma}$, and β is an unknown parameter associated with the accelerating variable. The quantity $x_{\max} = -11{,}605/[\max_i(\text{Temp}_i) + 273.16]$ is defined to be the transformed value of the highest level of the accelerating variable (i.e., temperature).

The distribution of the error terms ε_{ijk} is specified in (5), which follow normal distributions with standard deviation σ and correlation ρ. In particular, we consider a compound symmetric correlation structure for measurements taken on the same temperature and time point. The parameter ρ represents the within-batch correlation. In an ADDT, a batch of samples (e.g., five samples) is exposed to high temperature in the same test chamber for the same period of time. Thus, correlations can be introduced, for example, due to inaccuracy in controlling the testing temperature. Measurements at different temperature levels and time points are assumed to be independent.

The model in (3) falls within the class of scale-acceleration models. For a specific stress level i, $\mathcal{D}(t, x_i; \boldsymbol{\theta})$ is a decreasing function of time t, in which β controls the degradation rate through time-scale factor $\exp(\beta s_i)$ in (4). A smaller time-scale factor corresponds to a rapid decrease in degradation. When the acceleration level is at its highest, $s_{\max} = x_{\max} - x_{\max} = 0$. In this case, $\eta_i(t; \beta) = t$ implies that the degradation path no longer relies on β, and

$$\mathcal{D}(t, x_{\max}; \boldsymbol{\theta}) = g(t; \boldsymbol{\gamma}).$$

Thus, the function $g(\cdot)$ can be interpreted as the baseline degradation path for the scale-acceleration model in (3).

Let y_M be the lowest degradation level present in the observed data. Then the scale-acceleration model and the monotonicity of $g(\cdot)$ will allow one to extrapolate the degradation level to y_M for any given acceleration level. Let $\mathcal{D}_f$ be the failure threshold. Then, if $y_M < D_f$, one can use the semiparametric model to obtain failure information at the use condition through this extrapolation. This is particularly useful since, in general, measurements may be available below $\mathcal{D}_f$ for only some of the highest levels of the accelerating variable. In fact, some industrial standards require that tests be run until the degradation level drops below $\mathcal{D}_f$ for several acceleration levels. However, extrapolation beyond y_M is not possible due to the nonparametric construction of the $g(\cdot)$, which is the tradeoff for the model flexibility from nonparametric methods.

2.3 Nonparametric Form for Baseline Degradation Path

We use nonparametric methods to estimate the baseline degradation path $g(\cdot)$. Specifically, we use monotonic B-splines to model the baseline degradation path. This not only provides flexible models, but also retains the physical meaning of degradation mechanisms (e.g., the degradation path is monotone decreasing).

Consider a set of r interior knots $d_1 \leq \cdots \leq d_r$, and two boundary points d_0 and d_{r+1}. The entire set of ordered knots are

$$d_{-q} = \cdots = d_0 \leq d_1 \leq \cdots \leq d_r \leq d_{r+1} = \cdots = d_{r+q+1},$$

where the lower and upper boundary points are appended q times and q is the polynomial degree. For notational simplicity, we rewrite the subscripts in the ordered knot sequences as $d_1, \ldots, d_{r+2q+2}$. The total number of basis functions is $p = r + q + 1$, which is the length of parameter $\boldsymbol{\gamma}$. The lth B-spline basis function of degree q evaluated at z can be recursively obtained in the following formulas:

$$B_{0l}(z) = \mathbf{1}(d_l \leq z < d_{l+1}),$$

$$B_{ql}(z) = \frac{z - d_l}{d_{l+q} - d_l} B_{q-1,l}(z) + \frac{d_{l+q+1} - z}{d_{l+q+1} - d_{l+1}} B_{q-1,l+1}(z),$$

where $l = 1, \ldots, p$, and $\mathbf{1}(\cdot)$ is an indicator function. The degradation model can then be expressed as

$$y_{ijk} = \sum_{l=1}^{p} \gamma_l B_{ql}[\eta_i(t_{ij}; \beta)] + \varepsilon_{ijk}, \tag{6}$$

where γ_l's are the coefficients.

To ensure the degradation path is monotone decreasing, we require the first derivative of $\mathcal{D}(t, x_i; \boldsymbol{\theta})$ be a negative. For B-spline basis functions, De Boor (2001) proved that the derivative of $\mathcal{D}(t, x_i; \boldsymbol{\theta})$ with respect to $\eta_i(t; \beta)$ is

$$\frac{d\mathcal{D}(t, x_i; \boldsymbol{\theta})}{d\eta_i(t; \beta)} = \sum_{l=2}^{p} (q-1) \frac{(\gamma_l - \gamma_{l-1})}{d_{l+q+1} - d_l} B_{q-1,l}[\eta_i(t; \beta)].$$

As B-spline basis functions are nonnegative, it follows that $\gamma_l \leqslant \gamma_{l-1}$ for all $2 \leq l \leq p$ gives a sufficient condition for a monotone decreasing degradation path. However, except for basis functions with degree $q = 1, 2$, it is not a necessary condition. Fritsch and Carlson (1980) derived the necessary conditions for cubic splines ($q = 3$), though for higher order splines necessary conditions are as yet unclear.

3. Estimation and Inference

3.1 Parameter Estimation

Let $\boldsymbol{y}_{ij} = (y_{ij1}, \ldots, y_{ijn_{ij}})'$, $\boldsymbol{\varepsilon}_{ij} = (\varepsilon_{ij1}, \ldots, \varepsilon_{ijn_{ij}})'$, $\boldsymbol{y} = (\boldsymbol{y}'_{11}, \ldots, \boldsymbol{y}'_{1J_1}, \ldots, \boldsymbol{y}'_{n1}, \ldots, \boldsymbol{y}'_{nJ_n})'$, $\boldsymbol{\varepsilon} = (\boldsymbol{\varepsilon}'_{11}, \ldots, \boldsymbol{\varepsilon}'_{1J_1}, \ldots, \boldsymbol{\varepsilon}'_{n1}, \ldots, \boldsymbol{\varepsilon}'_{nJ_n})'$, and $\boldsymbol{\gamma} = (\gamma_1, \ldots, \gamma_p)'$. The degradation model in (6) can be written as

$$\boldsymbol{y} = \mathbf{X}_\beta \boldsymbol{\gamma} + \boldsymbol{\varepsilon}, \tag{7}$$

where

$$\mathbf{X}_\beta = \begin{bmatrix} B_{q1}[\eta_1(t_{11}; \beta)] & \cdots & B_{qp}[\eta_1(t_{11}; \beta)] \\ B_{q1}[\eta_1(t_{12}; \beta)] & \cdots & B_{qp}[\eta_1(t_{12}; \beta)] \\ \vdots & \ddots & \vdots \\ B_{q1}[\eta_n(t_{nJ_n}; \beta)] & \cdots & B_{qp}[\eta_n(t_{nJ_n}; \beta)] \end{bmatrix},$$

and $\boldsymbol{\varepsilon} \sim \mathrm{N}(\mathbf{0}, \boldsymbol{\Sigma})$. Here, $\boldsymbol{\Sigma} = \mathrm{Diag}(\boldsymbol{\Sigma}_{11}, \ldots, \boldsymbol{\Sigma}_{1J_1}, \ldots, \boldsymbol{\Sigma}_{n1}, \ldots, \boldsymbol{\Sigma}_{nJ_n})$ and $\boldsymbol{\Sigma}_{ij} = \sigma^2[(1-\rho)\boldsymbol{I}_{n_{ij}} + \rho \boldsymbol{J}_{n_{ij}}]$, where $\boldsymbol{I}_{n_{ij}}$ is an $n_{ij} \times n_{ij}$ identity matrix and $\boldsymbol{J}_{n_{ij}}$ is an $n_{ij} \times n_{ij}$ matrix of 1's. We can also rewrite $\boldsymbol{\Sigma} = \sigma^2 \boldsymbol{R}$, where $\boldsymbol{R} = \mathrm{Diag}(\boldsymbol{R}_{11}, \ldots, \boldsymbol{R}_{1J_1}, \ldots, \boldsymbol{R}_{n1}, \ldots, \boldsymbol{R}_{nJ_n})$ and $\boldsymbol{R}_{ij} = (1-\rho)\boldsymbol{I}_{n_{ij}} + \rho \boldsymbol{J}_{n_{ij}}$.

We use likelihood-based methods to estimate the unknown parameters $\boldsymbol{\theta} = (\boldsymbol{\gamma}', \beta, \sigma, \rho)'$. For now, we consider estimation of $\boldsymbol{\theta}$ with a given number of knots and knot locations. We will give a discussion on knots selection in Section 3.3. A particular challenge to the estimation comes from the constraints on $\boldsymbol{\gamma}$, namely, that $\gamma_l \leq \gamma_{l-1}$, $2 \leq l \leq p$. We also note that, for a given β, $\mathbf{X}_\beta$ is known, in which case (7) becomes a linear model with a correlated covariance structure. Thus, we proceed by first deriving estimates of $(\boldsymbol{\gamma}', \sigma, \rho)'$ given β and then use a profile likelihood approach to estimate β.

The estimates of $\boldsymbol{\gamma}$ and $(\sigma, \rho)'$ are obtained using an iterative procedure. In particular, at the mth iteration, given estimates $(\widehat{\sigma}^{(m-1)}, \widehat{\rho}^{(m-1)})'$, the value of $\widehat{\boldsymbol{\gamma}}^{(m)}$ is obtained by minimizing

$$Q(\boldsymbol{\gamma}) = (\boldsymbol{y} - \mathbf{X}_\beta \boldsymbol{\gamma})' \left(\widehat{\boldsymbol{\Sigma}}^{(m-1)}\right)^{-1} (\boldsymbol{y} - \mathbf{X}_\beta \boldsymbol{\gamma})$$
$$\text{subject to } \gamma_l \leqslant \gamma_{l-1}, 2 \leq l \leq p. \tag{8}$$

Equation (8) is a quadratic object function with linear constraints. So it can be solved with quadratic programming techniques such as the dual method in Goldfarb and Idnani (1983) and the Hinge algorithm in Meyer (2013). In this article, the Hinge algorithm is used.

With the estimate $\widehat{\boldsymbol{\gamma}}^{(m)}$, one can then obtain $(\widehat{\sigma}^{(m)}, \widehat{\rho}^{(m)})'$ using restricted maximum likelihood (REML) as long as $\widehat{\boldsymbol{\gamma}}^{(m)}$ does not take values on the boundary of the linear constraints. If the solution of (8) takes values on the boundary of the linear constraints, we use approximate REML to update estimates of σ and ρ. In particular, let $\widehat{\boldsymbol{\gamma}}_u^{(m)}$ represent all of the unique values in $\widehat{\boldsymbol{\gamma}}^{(m)}$ and p_u be the length of $\widehat{\boldsymbol{\gamma}}_u^{(m)}$. For each unique value $\widehat{\gamma}_{i,u}^{(m)}$, let $\boldsymbol{x}_{i,\beta u}$ be the sum of the corresponding columns in $\mathbf{X}_\beta$. Then we have $\mathbf{X}_\beta \widehat{\boldsymbol{\gamma}}^{(m)} = \mathbf{X}_{\beta u} \widehat{\boldsymbol{\gamma}}_u^{(m)}$, where $\mathbf{X}_{\beta u} = (\boldsymbol{x}_{1,\beta u}, \ldots, \boldsymbol{x}_{p_u,\beta u})$. The approximate REML log-likelihood is

$$\mathcal{L}_{\mathrm{REML}}(\sigma, \rho | \widehat{\boldsymbol{\gamma}}^{(m)}) = -\frac{1}{2}\Big\{ \log|\boldsymbol{\Sigma}| + \log|\mathbf{X}'_{\beta u} \boldsymbol{\Sigma}^{-1} \mathbf{X}_{\beta u}| + \left(\boldsymbol{y} - \mathbf{X}_\beta \widehat{\boldsymbol{\gamma}}^{(m)}\right)' \boldsymbol{\Sigma}^{-1} \left(\boldsymbol{y} - \mathbf{X}_\beta \widehat{\boldsymbol{\gamma}}^{(m)}\right) \Big\}. \tag{9}$$

The covariance parameter estimates $(\widehat{\sigma}^{(m)}, \widehat{\rho}^{(m)})'$ are those values that maximize (9). In particular, after some calculation it can be shown that $\widehat{\sigma}^{(m)}$ has the following closed-form expression

$$\widehat{\sigma}^{(m)} = \left[\frac{(\boldsymbol{y} - \mathbf{X}_\beta \widehat{\boldsymbol{\gamma}}^{(m)})' (\widehat{\boldsymbol{R}}^{(m-1)})^{-1} (\boldsymbol{y} - \mathbf{X}_\beta \widehat{\boldsymbol{\gamma}}^{(m)})}{N - p_u} \right]^{\frac{1}{2}}.$$

Thus, $\widehat{\rho}^{(m)}$ can be obtained from a one-dimensional optimization problem. That is,

$$\widehat{\rho}^{(m)} = \underset{\rho}{\mathrm{argmax}} \Big\{ -\log|(\widehat{\sigma}^{(m)})^2 \boldsymbol{R}| - \log|(\widehat{\sigma}^{(m)})^{-2} \mathbf{X}'_{\beta u} \boldsymbol{R}^{-1} \mathbf{X}_{\beta u}| - (\widehat{\sigma}^{(m)})^{-2} \left(\boldsymbol{y} - \mathbf{X}_\beta \widehat{\boldsymbol{\gamma}}^{(m)}\right)' \boldsymbol{R}^{-1} \left(\boldsymbol{y} - \mathbf{X}_\beta \widehat{\boldsymbol{\gamma}}^{(m)}\right) \Big\}.$$

Upon convergence, the estimates of $(\widehat{\boldsymbol{\gamma}}', \widehat{\sigma}, \widehat{\rho})'$ are obtained for a given β, denoted by $(\widehat{\boldsymbol{\gamma}}'_\beta, \widehat{\sigma}_\beta, \widehat{\rho}_\beta)'$. The initial values $(\widehat{\sigma}^{(0)}, \widehat{\rho}^{(0)})'$ can be easily obtained by fitting a nonconstrained model.

The profile log-likelihood for β is given as

$$\mathcal{L}(\beta, \widehat{\boldsymbol{\gamma}}_\beta, \widehat{\sigma}_\beta, \widehat{\rho}_\beta) = \log \left\{ \frac{1}{(2\pi)^{N/2} |\widehat{\boldsymbol{\Sigma}}_\beta|^{1/2}} \exp\left[-\frac{(\boldsymbol{y} - \mathbf{X}_\beta \widehat{\boldsymbol{\gamma}}_\beta) \widehat{\boldsymbol{\Sigma}}_\beta^{-1} (\boldsymbol{y} - \mathbf{X}_\beta \widehat{\boldsymbol{\gamma}}_\beta)}{2} \right] \right\}.$$

In practice, one can first estimate $(\boldsymbol{\gamma}', \sigma, \rho)'$ for a specified range of values of β, then compute $\mathcal{L}(\beta, \widehat{\boldsymbol{\gamma}}_\beta, \widehat{\sigma}_\beta, \widehat{\rho}_\beta)$ as a function of β. The estimate $\widehat{\beta}$ is the value that maximizes this function. The final estimates are denoted by $\widehat{\boldsymbol{\theta}} = (\widehat{\boldsymbol{\gamma}}', \widehat{\beta}, \widehat{\sigma}, \widehat{\rho})'$.

Here, we provide some discussion on the estimation procedure. Regarding the convergence of the algorithm, the likelihood

function is the same as the likelihood function of a linear mixed model with a given β. The restrictions on $\boldsymbol{\gamma}$ reduce the parameter space but that does not change the shape of the likelihood function. The parameter β is related to the acceleration rate, which can be determined by the data from different levels of temperature. If the value of β is too large or too small, a smaller likelihood value will result. That is, a certain finite value of β will maximize the likelihood value. Thus, the algorithm converges well as long as there is enough information on the acceleration rate from the data, which typically requires three levels for the temperature. To specify the initial range of β, one can fit polynomial curves (e.g., third-order polynomial) separately to the data from each temperature level. By comparing the time to reach a certain degradation level (e.g., 70% of the original strength) at different temperature levels, one can obtain several rough estimates of β. The range of these estimates can be used to specify the initial range of β.

3.2 Reliability Measures

Once the model parameters are estimated, other parameters related to reliability can then be estimated. For example, the mean time to failure (MTTF), denoted by μ_f, is one of ways to evaluate the reliability of a product/material. Based on the semiparametric model, we can derive an estimate $\widehat{\mu}_f$ at a use condition x_f and failure threshold $\mathcal{D}_f$ by solving

$$\mathcal{D}(\widehat{\mu}_f, x_f; \widehat{\boldsymbol{\theta}}) = \sum_{l=1}^{p} \widehat{\gamma}_l B_{ql}\left(\frac{\widehat{\mu}_f}{\exp[\widehat{\beta}(x_{\max} - x_f)]}\right) = \mathcal{D}_f.$$

We can also derive the failure time distribution from the semiparametric model. The event that the failure time T is less than t (i.e., $T \le t$) is equivalent to that the degradation measurement at time t is less than the failure threshold $\mathcal{D}_f$ (i.e., $y_t \le \mathcal{D}_f$), for monotonic decreasing degradation paths. Here, y_t is the degradation measurement at t. Hence, the cumulative distribution function (cdf) of failure time, $F_T(t)$, can be calculated as

$$\begin{aligned} F_T(t) &= P(T \le t) = P(y_t \le D_f) \\ &= \Phi\left(\frac{\mathcal{D}_f - g[\frac{t}{\exp(\beta s)}; \boldsymbol{\gamma}]}{\sigma}\right), \quad t \geqslant 0, \end{aligned}$$

where $\Phi(\cdot)$ is the cdf of the standard normal distribution. The quantile function can then be calculated as the inverse of the cdf. That is, the α quantile is $t_\alpha = F_T^{-1}(\alpha)$. In the case of no closed-form expression, numerical methods can be used to find the quantile function from the cdf.

3.3 Spline Knots Selection

The number of knots and knot locations are a key component to using B-splines to model the degradation path. In addition, it is also necessary to determine the maximum degree of the B-splines. For knot selection, we first fix the degree of the B-splines and then find the optimum knot locations. Optimality is determined by a variation of the Akaike information criterion:

$$\text{AIC} = -2\log\left\{\frac{1}{(2\pi)^{N/2}|\widehat{\boldsymbol{\Sigma}}|^{1/2}}\exp\left[-\frac{(\boldsymbol{y} - \mathbf{X}_{\widehat{\beta}}\widehat{\boldsymbol{\gamma}})\widehat{\boldsymbol{\Sigma}}^{-1}(\boldsymbol{y} - \mathbf{X}_{\widehat{\beta}}\widehat{\boldsymbol{\gamma}})}{2}\right]\right\} + 2 \times \text{edf}, \tag{10}$$

where edf is the effective degrees of freedom in $\boldsymbol{\gamma}$ plus three for the parameters $(\beta, \sigma, \rho)'$. Wang, Meyer, and Opsomer (2013) and Meyer (2012) discussed constrained spline regression for both independent and correlated error cases. In particular, they showed how to calculate the effective degrees of freedom for a constrained fit through the use of a cone projection, which is the trace of the projection matrix. Because we have $p - 1$ linear constraints, the effective degrees of freedom in $\boldsymbol{\gamma}$ has a value from 1 to p, where p corresponds to an unconstrained fit. Letting q denote the degree of the B-spline functions, the procedure for knot selection is as follows:

1. Determine the optimal number of interior knots $r_{\text{opt},q}$, which minimizes the AIC. The default knot locations are equally spaced sample quantiles. That is, if the number of interior knots is r, the default knot locations are b/r, $b = 1, \ldots, r - 1$.
2. Delete each of the internal knots in sequence. The knot whose deletion leads to the greatest reduction in AIC is removed. Repeat until no more existing knots can be removed.

The whole procedure is to be repeated for different B-spline degrees until the optimal knot sequence is determined. This knot selection procedure is similar to the procedure in He and Shi (1998). The sample size for an ADDT is typically small and so a low degree of spline ($q \leqslant 4$) and a small number of interior knots ($1 \leqslant r \leqslant 5$) are usually sufficient to provide a good fit to the data.

3.4 Statistical Inference

Inference based on the semiparametric model in (7) can rely on either asymptotic theory or a bootstrap procedure. Because the bootstrap method is straightforward and easy to implement, we use a nonparametric bootstrap to calculate confidence intervals (CI) for the parameters and pointwise CI for the degradation path. The error term in model (7) can be written as

$$\varepsilon_{ijk} = u_{ij} + e_{ijk},$$

where $u_{ij} \sim \text{N}(0, \sigma_u^2)$, $e_{ijk} \sim \text{N}(0, \sigma_e^2)$, $\text{Corr}(u_{ij}, e_{ijk}) = 0$, $\sigma_u^2 = \rho\sigma^2$, and $\sigma_e^2 = (1 - \rho)\sigma^2$. That is, the error term in model (7) can be written as the sum of a random effect term u_{ij} and an independent error term e_{ijk}. To obtain the CI, one could resample from the estimated random effect term $\widehat{u}_{ij}$ and the estimated independent error term $\widehat{e}_{ijk}$ separately. However, Carpenter, Goldstein, and Rasbash (2003) showed that directly resampling from $\widehat{u}_{ij}$ and $\widehat{e}_{ijk}$ will cause bias. Therefore, we adjust $\widehat{u}_{ij}$ and $\widehat{e}_{ijk}$ prior to bootstrapping. That is,

$$\widehat{u}_{ij}^c = \left[\sum_{ij}\widehat{u}_{ij}^2 \Big/ \sum_{i=1}^{n} J_i\right]^{-1/2} \widehat{\sigma}_u \widehat{u}_{ij}, \quad \text{and}$$

$$\widehat{e}_{ijk}^c = \left[\sum_{k}\widehat{e}_{ijk}^2 \Big/ n_{ij}\right]^{-1/2} \widehat{\sigma}_e \widehat{e}_{ijk}.$$

The specific steps of the nonparametric bootstrap are described as follows:

1. Sample $u_{ij}^{c(m)}$ with replacement from $\widehat{u}_{ij}^{c}$ and sample $e_{ijk}^{c(m)}$ with replacement from $\widehat{e}_{ijk}^{c}$.
2. Compute $y_{ijk}^{(m)} = x_{ij}'\widehat{\boldsymbol{\gamma}} + u_{ij}^{c(m)} + e_{ijk}^{c(m)}$.
3. Fit the semiparametric model to the bootstrapped samples $y_{ijk}^{(m)}$, $m = 1, \ldots, B$.

Let θ be a general notation for a parameter to be estimated. For a sequence of ordered bootstrap estimates $\widehat{\theta}^{(1)}, \ldots, \widehat{\theta}^{(B)}$, the quantile-based CI with confidence level $1-\alpha$ for θ is calculated by taking the lower and upper $\alpha/2$ quantiles of the bootstrap estimates. That is $(\widehat{\theta}^{([B\alpha/2])}, \widehat{\theta}^{([B(1-\alpha/2)])})$, where $[\cdot]$ is the rounding function. A bias-corrected CI, proposed by Efron and Tibshirani (1993), can be computed by taking the $[B\Phi(2z_\zeta + z_{\alpha/2})]$th and $[B\Phi(2z_\zeta + z_{1-\alpha/2})]$th ordered values. That is $(\widehat{\theta}^{([B\Phi(2z_\zeta+z_{\alpha/2})])}, \widehat{\theta}^{([B\Phi(2z_\zeta+z_{1-\alpha/2})])})$. Here, ζ denotes the proportion of the bootstrap values that are less than $\widehat{\theta}$, and $\Phi(\cdot)$ and z_α are the cdf and the α quantile of the standard normal distribution, respectively.

4. SIMULATION STUDY

The objective of the simulation study is to investigate the performance of the proposed parameter estimation and inference procedures. We will examine the bias, standard deviation (SD), and mean squared error (MSE) of estimators of the parameters and the baseline degradation function. We also will investigate the coverage probability (CP) of the bootstrap-based CI procedure in Section 3.4. An additional simulation study will be conducted to investigate the performance of the proposed semiparametric model under model misspecification.

4.1 Performance of Parameter Estimators

4.1.1 Simulation Settings

We consider two different values for the temperature levels (i.e., $n = \{3, 6\}$). To simplify the setting, the measuring time points are set to be the same for all temperature levels. We consider three different values for the number of measuring times, denoted by $J_n = \{5, 10, 15\}$. Thus, we have six combinations of temperature levels and the number of measuring time points in the simulation. The specific settings are summarized in Table 1. Ten samples are tested at each combination of temperature level and measuring times. The data are simulated from the following model:

Table 1. Selected temperature levels and time points for the simulation studies.

Settings	Number of temp. levels (n)	Temperature levels (°C)
Temperature setting 1	3	50, 65, 80
Temperature setting 2	6	30, 40, 50, 60, 70, 80
	Number of time points (J_n)	Measuring times (Days)
Time point setting 1	5	8, 25, 75, 130, 170
Time point setting 2	10	5, 10, 30, 50, 70, 90, 110, 130, 150, 170
Time point setting 3	15	10, 30, 40, 50, 60, 70, 80, 90, 100, 110, 120, 130, 140, 150, 170

$$y_{ijk} = \mathcal{D}(t_{ij}, x_i; \boldsymbol{\theta}) + \varepsilon_{ijk} = \sum_{l=1}^{p} r_l B_{ql}[\eta_i(t_{ij}; \beta)] + \varepsilon_{ijk}, \quad (11)$$

where the degree of the B-splines is $q = 2$, and number of interior knots is $r = 3$. The knot locations are the sample quantiles. Figure 1 gives the spline basis functions and the baseline degradation function for the scenario with $n = 3$ and $J_n = 5$. The true parameters in the model are $\beta = 0.83$, $\boldsymbol{\gamma} = (1, 0.9, 0.8, 0.7, 0.6, 0.6)'$, and $(\sigma, \rho)' = (0.019, 0.2)'$.

For each scenario, 500 datasets are generated and the bias, SD, and MSE of the estimators of parameters and baseline degradation curves are calculated. The quantile-based and bias-corrected CI are computed based on $B = 1000$ bootstrap samples and the CP is also computed.

4.1.2 Simulation Results

Figure 2 shows the bias and MSE of parameter estimators. Figure 3 shows the pointwise MSE curves of baseline degradation curves. We find that the MSE of the point estimators and baseline degradation curve estimators decrease as either the number of temperature levels or time points increases. Even when the number of temperature levels and time points are both small, biases of β and σ are small, while the bias of ρ is large. When either the number of temperature levels or time points is

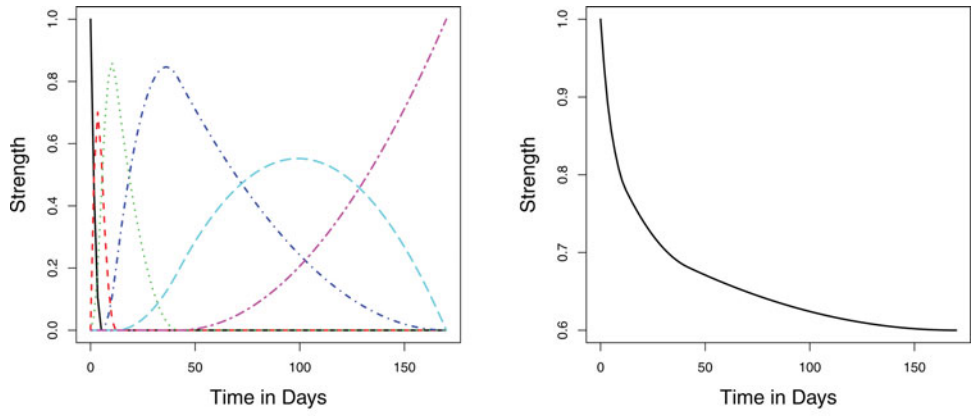

(a) Spline bases (b) Baseline degradation path

Figure 1. Spline bases and baseline degradation path used in simulation study.

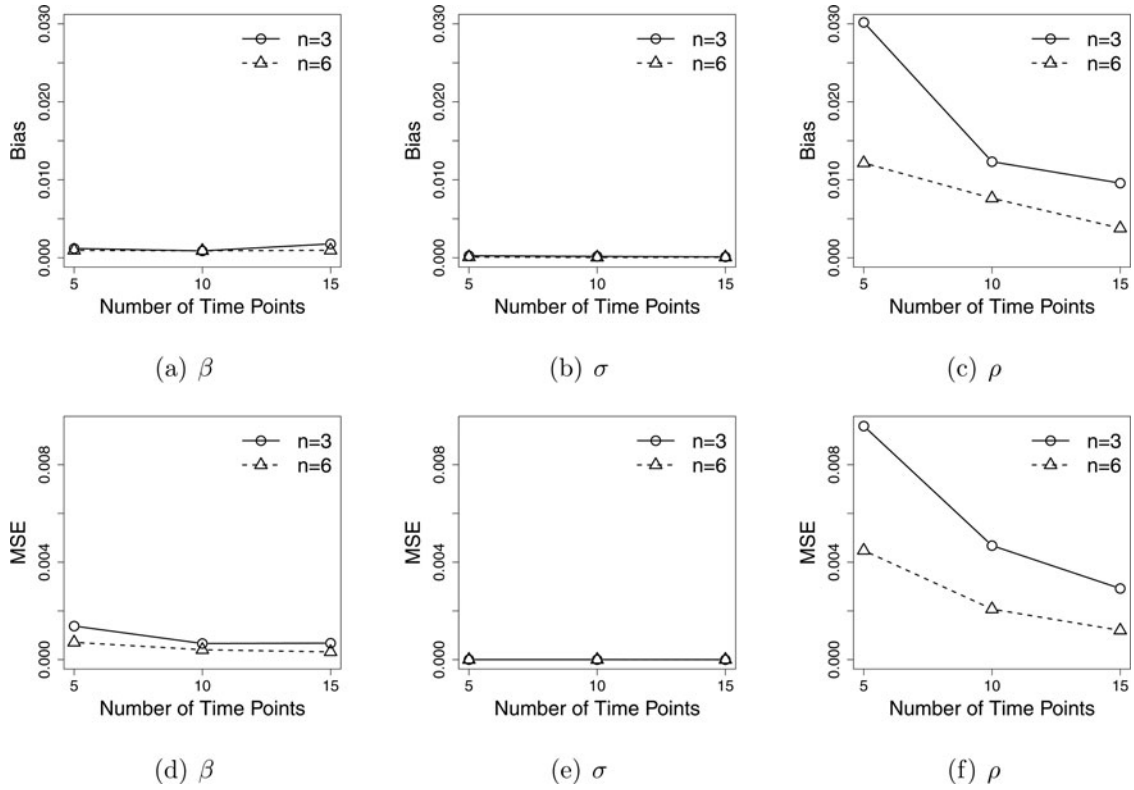

Figure 2. Empirical bias and MSE of parameter estimators for $(\beta, \sigma, \rho)'$.

large, the estimates of β, σ, and ρ are all close to the true values. We also observe some increasing/decreasing trends of the MSE plot in Figure 3. The majority of the curves, however, fall within 2×10^{-5} and 8×10^{-5}, which is quite a small range. The underlying reason for such fluctuation is that we no longer have an adequate number of interior knots for those time periods near the end of experiment.

Figures 4 and 5 present the CP for quantile-based CI and bias-corrected CI of the parameters and baseline degradation curves. The performance of bias-corrected CI is similar for β, and better for σ, ρ and the baseline degradation curve compared to quantile-based CI. For the parameter estimators, the CP of bias-corrected CI of β is good when n or J_n is small. However, the CP of bias-corrected CI of $(\sigma, \rho)'$ are overall slightly less than the desired confidence level. For the baseline degradation function, the CP of pointwise bias-corrected CI are poor when $n = 3$ and $J_n = 5$. The performance of pointwise bias-corrected CI improves as n and J_n increase. Overall, the results show that the performance of the estimation and inference procedures are good.

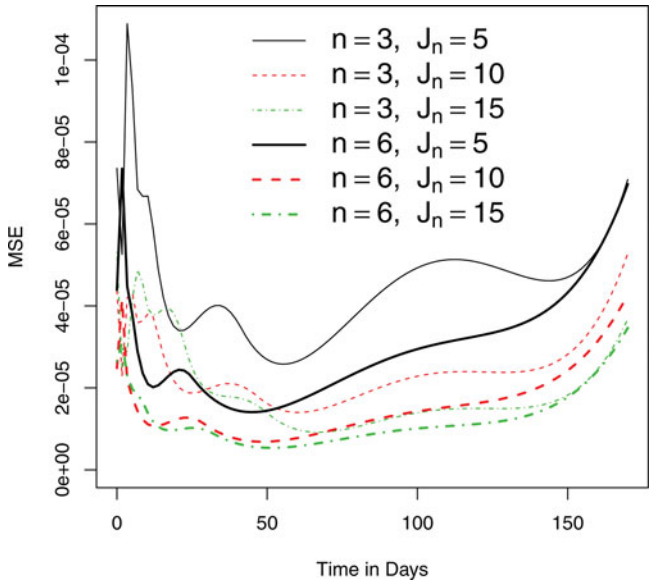

Figure 3. Empirical pointwise MSE for the estimator of the baseline degradation path.

4.2 Performance Under Model Misspecification

4.2.1 Simulation Settings

In this simulation study, the data are simulated according to a parametric model. Then, the semiparametric model is used to fit the simulated data. The temperature levels are set at 50°C, 65°C, 80°C and the measuring times are set at 192, 600, 1800, 3120, and 4320 hr. There are 10 samples measured at time 0 and 5 samples measured at all other time points. The data are simulated from the model

$$y_{ijk} = \beta_0 + \beta_1 \exp(\beta_2 x_i) t_{ij} + \varepsilon_{ijk}, \tag{12}$$

where Temp_i is the ith temperature level, t_{ij} is the jth measuring time point for temperature level i, and $x_i = -11,605/(\text{Temp}_i + 273.15)$. The true parameters are $\boldsymbol{\beta} = (\beta_0, \beta_1, \beta_2)' = (1, -3.5, 0.3)'$, and $(\sigma, \rho)' = (0.02, 0)'$. In practice, the true model may not be known exactly. Thus, we also consider the case when a different parametric model from the true one is used to fit the data. The incorrect parametric model, adapted from Vaca-Trigo and Meeker (2009), is given

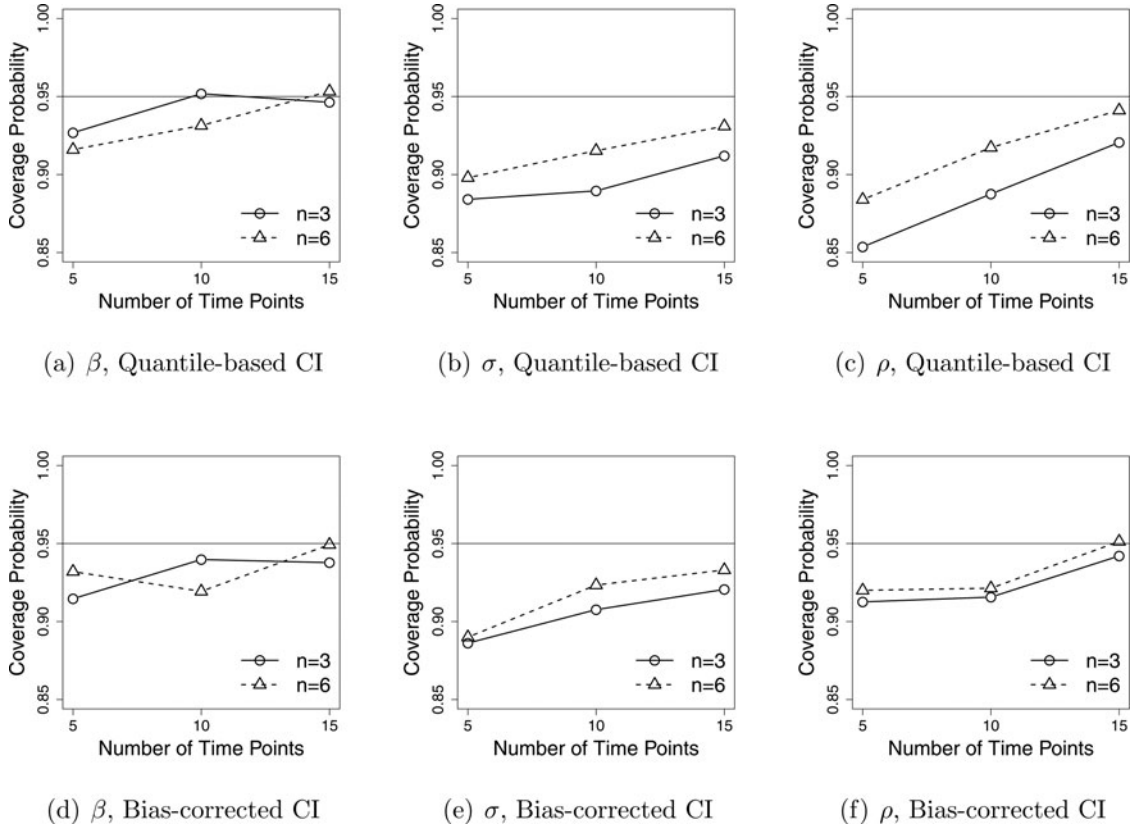

(a) β, Quantile-based CI (b) σ, Quantile-based CI (c) ρ, Quantile-based CI

(d) β, Bias-corrected CI (e) σ, Bias-corrected CI (f) ρ, Bias-corrected CI

Figure 4. CP of the CI procedures for parameters $(\beta, \sigma, \rho)'$, using quantile-based and bias-corrected methods, respectively.

by

$$y_{ijk} = \frac{\alpha_0}{1 + [\frac{t_{ij}}{\exp(\beta_0 + \beta_1 x_i)}]^{\gamma}} + \varepsilon_{ijk}, \tag{13}$$

with parameters $(\alpha_0, \beta_0, \beta_1, \gamma)'$ in the mean structure. We fit the true model (12), the incorrect parametric model (13), and the semiparametric model (3) to the simulated data. Figure 6 shows one case of the simulated data and the fitted degradation paths. The semiparametric model can follow the path of the true model closely.

4.2.2 Simulation Results

To assess the fit of the proposed semiparametric model, we compare the fitted degradation path to the true degradation path using the integrated mean squared error (IMSE) of the baseline degradation function estimator, which is defined as

$$\begin{aligned} \text{IMSE} &= \int_0^{t_m} \mathbf{E}\left\{\left[\widehat{g}(t;\boldsymbol{\gamma}) - g(t;\boldsymbol{\gamma})\right]^2\right\} dt \\ &= \int_0^{t_m} \left\{\mathbf{E}\left[\widehat{g}(t;\boldsymbol{\gamma})\right] - g(t;\boldsymbol{\gamma})\right\}^2 dt + \int_0^{t_m} \text{Var}\left[\widehat{g}(t;\boldsymbol{\gamma})\right] dt \\ &= \text{IBias}^2 + \text{IVar}, \end{aligned}$$

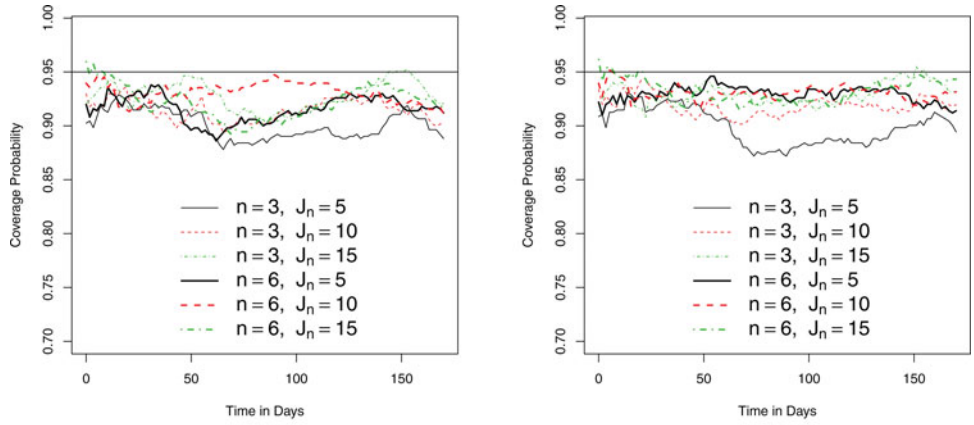

(a) Quantile-based CI (b) Bias-corrected CI

Figure 5. Pointwise CP of the CI procedure for baseline degradation path, using quantile-based and bias-corrected methods, respectively.

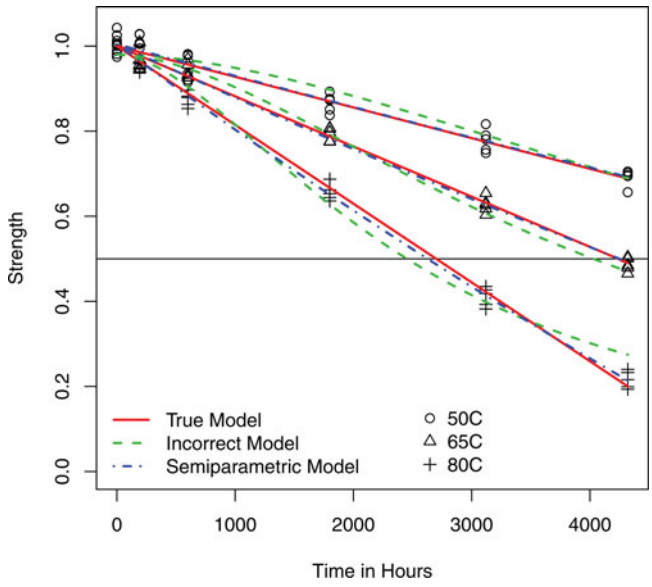

Figure 6. Plot of a simulated dataset and fitted degradation paths based on the true and incorrect parametric models, and the semiparametric model.

where t_m is the maximum time under the maximum level of the accelerating variable. As there is no closed-form expressions for IMSE, integrated squared bias (IBias^2), and integrated variance (IVar), we report the empirical results. Table 2 presents these results, which indicate that the performance of the proposed semiparametric model is good. The largest contribution to the root IMSE comes from the variance component. Thus, it is not surprising that the incorrect parametric model (13) performs the worst in capturing the true degradation path.

For each simulated dataset, the MTTF at 30°C (the normal use condition specified in the simulation setting) is calculated based on the true parametric model (12), the incorrect parametric model (13), and the semiparametric model. The mean, bias, standard derivation (SD), and root MSE of the MTTF for each of the different models based on 600 datasets are summarized in Table 3. The results indicate that the estimate of MTTF from the semiparametric model is close to the true value, but with larger variance when compared to other models, which is due to the larger number of parameters that need to be estimated. The estimated MTTF from the incorrect parametric model (13) has the largest bias, leading to a larger RMSE. The results indicate the proposed semiparametric model performs quite well.

Table 2. Empirical IBias, root IVar (RIVar), and root IMSE (RIMSE) for the true model (12), the incorrect model (13), and the semiparametric model.

Models	IBias	RIVar	RIMSE
True model	0.0003	0.0043	0.0043
Incorrect model	0.0267	0.0060	0.0274
Semiparametric model	0.0003	0.0091	0.0091

Table 3. Empirical mean, bias, SD, and root MSE (RMSE) of the MTTF estimators based on the true model (12), the incorrect model (13), and the semiparametric model.

Models	Mean	Bias	SD	RMSE
True model	82.60	0.01	2.99	2.99
Incorrect model	85.82	3.20	3.75	4.93
Semiparametric model	82.77	0.16	4.22	4.22

5. Applications

To help motivate the use of the proposed semiparametric model, we selected three published datasets from well-known examples of ADDT. The data for each example are summarized below.

5.1 ADDT Datasets and Parametric Models

5.1.1 The Adhesive Bond B Data

Escobar et al. (2003) discussed an experiment that measured the strength of an adhesive bond (Adhesive Bond B) over time. Eight units were measured at the beginning of the experiment under normal temperature to serve as the baseline strength. The remaining measurements were taken at selected weeks (2, 4, 6, 12, and 16) for three accelerated temperature levels (50°C, 60°C, and 70°C). A scatterplot of the Adhesive Bond B dataset is presented in Figure 7(a). The degradation model used by Escobar et al. (2003) is

$$y_{ijk} = \beta_0 + \beta_1 \exp(\beta_2 x_i)\tau_{ij} + \varepsilon_{ijk}, \tag{14}$$

where y_{ijk} is the strength of Adhesive Bond B in log Newtons, $\tau_{ij} = \sqrt{t_{ij}}$, $x_i = -11,605/(\text{Temp}_i + 273.15)$ is the Arrhenius-transformed temperature, and $\varepsilon_{ijk} \sim \text{N}(0, \sigma^2)$. The estimates are $\widehat{\beta}_0 = 4.4713$, $\widehat{\beta}_1 = -8.6384 \times 10^8$, $\widehat{\beta}_2 = 0.6364$, and $\widehat{\sigma} = 0.1609$.

5.1.2 The Seal Strength Data

Li and Doganaksoy (2014) considered a dataset from an ADDT test of seal strength. At the start of the experiment, a batch of 10 seal samples were measured at the use temperature level of 100°C. A batch of 10 seal samples were then tested at selected weeks (5, 10, 15, 20, and 25) for four temperature levels (200°C, 250°C, 300°C, and 350°C). A scatterplot of the seal strength data is shown in Figure 8(a). Though one would expect the seal strength to decrease under higher temperature, some batches of seal samples yielded higher strengths in later weeks compared with the initial measurements. This suggests a large batch-to-batch variability, which must be incorporated into the model. Thus, Li and Doganaksoy (2014) considered the following nonlinear mixed model:

$$y_{ijk} = \beta_0 - \beta_1 \exp(\beta_2 x_i)t_{ij} + \delta_{ij} + \varepsilon_{ijk}, \tag{15}$$

where y_{ijk} is the $\log_{10}$ strength of seal sample, and $x_i = -11,605/(\text{Temp}_i + 273.15)$. The random variable $\delta_{ij} \sim \text{N}(0, \sigma_\delta^2)$ represents batch-to-batch variability, $\varepsilon_{ijk} \sim \text{N}(0, \sigma^2)$, and δ_{ij} and ε_{ijk} are independent. The estimates are $\widehat{\beta}_0 = 1.4856$, $\widehat{\beta}_1 = 47.2166$, $\widehat{\beta}_2 = 0.3420$, $\widehat{\sigma} = 0.1603$, and $\widehat{\sigma}_\delta = 0.0793$.

5.1.3 The Adhesive Formulation K Data

A new adhesive, Formulation K, was developed and tested at 40°C, 50°C, and 60°C. The strength of 10 units was measured at the beginning of the experiment and a specified number of samples were tested at 3, 6, 12, 18, and 24 weeks. Figure 9(a) is a scatterplot of the data. The parametric model used to describe the data is

$$y_{ijk} = \log(90) + \beta_0 \left(1 - \exp\left\{-\beta_1 \exp\left[\beta_2 (x_i - x_2)\right] t_{ij}\right\}\right) + \varepsilon_{ijk}, \tag{16}$$

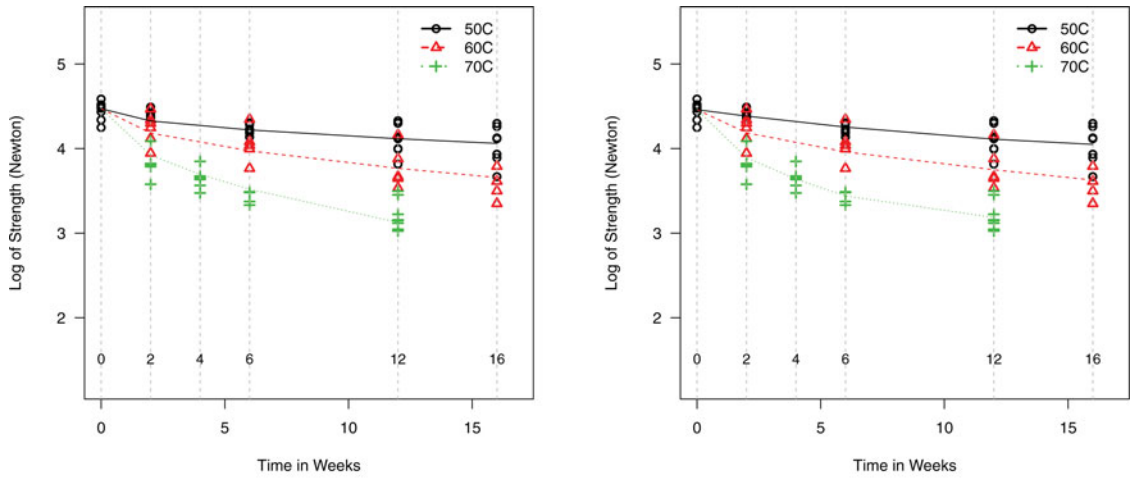

(a) Parametric model (b) Semi-parametric model

Figure 7. Fitted degradation paths of the Adhesive Bond B data.

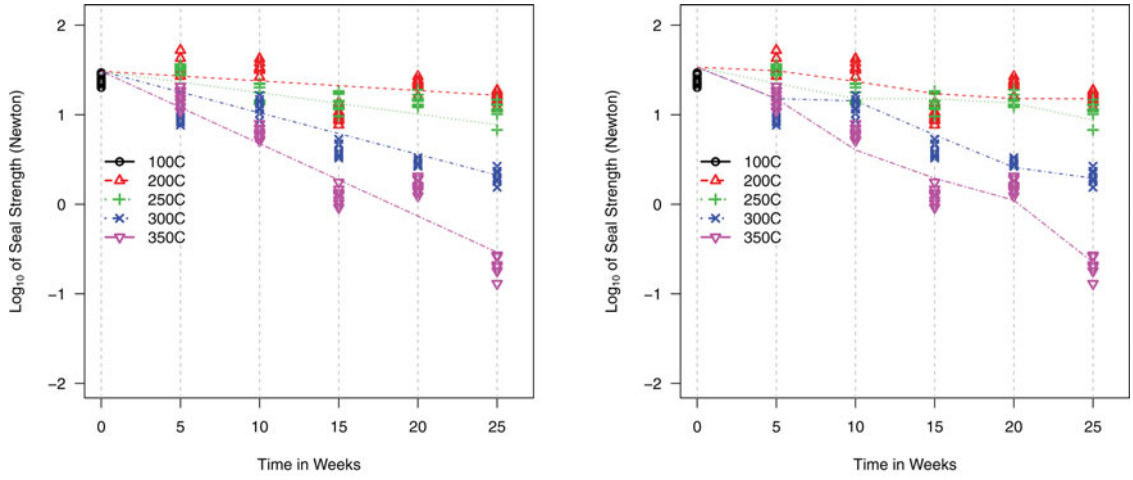

(a) Parametric model (b) Semi-parametric model

Figure 8. Fitted degradation paths of the seal strength data.

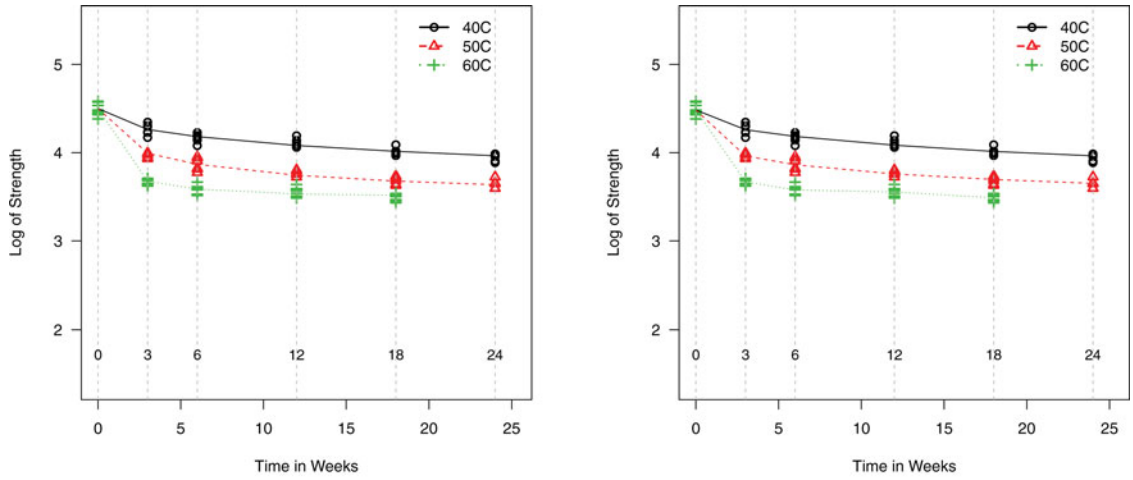

(a) Parametric model (b) Semi-parametric model

Figure 9. Fitted degradation paths of the adhesive formulation K data.

Table 4. Parameter estimates and corresponding 95% quantile-based CI for the semiparametric models for the three applications.

			Quantile-based CI	
Applications	Parameter	Estimate	95% lower	95% upper
Adhesive bond B	β	1.3422	1.1071	1.6165
	σ	0.1537	0.1265	0.1787
Seal strength	β	0.3235	0.2451	0.5194
	σ	0.1610	0.1192	0.1904
	ρ	0.7573	0.5465	0.8307
Adhesive formulation K	β	1.8221	1.6575	2.3658
	σ	0.0484	0.0419	0.0544

where y_{ijk} is the strength of adhesive formulation K in log Newtons, $\tau_{ij} = \sqrt{t_{ij}}$, $x_i = -11,605/(\text{Temp}_i + 273.15)$, $x_2 = -11,605/(50 + 273.15)$, and $\varepsilon_{ijk} \sim \text{N}(0, \sigma^2)$. The estimates are $\widehat{\beta}_0 = -0.9978$, $\widehat{\beta}_1 = 0.4091$, $\widehat{\beta}_2 = 0.8371$, and $\widehat{\sigma} = 0.0501$.

5.2 Comparisons of Parametric and Semiparametric Models

In this section, we also applied the developed method to each of the datasets. We applied the knot selection technique in Section 3.3 for each application. We also tested the significance of $\rho = 0$, which informs the selection of the appropriate model. The parameter estimates and their associated quantile-based CI are presented in Table 4.

To assess the fit of the semiparametric model and compare it with the corresponding parametric model chosen by the respective applications, we investigate the AIC values as defined in Section 3.3. In the calculation of AIC, the log-likelihood is the marginal log-likelihood for the parametric models. Table 5 contains the log-likelihood values, edf, and AIC for each model and dataset. For all three datasets, the semiparametric models possessed a lower AIC as compared to the parametric models. This indicates that the semiparametric model can provide a better description for the ADDT data.

We also compared the MTTF estimation using parametric and semiparametric models for the three applications. Table 6 shows the estimated MTTF and the associated 95% quantile-based CI at normal use conditions. For illustrations, the failure threshold is set to be 70% and the time is in weeks. For the adhesive bond B and adhesive formulation K data, the MTTF from the two models are close to each other. For the seal strength data, there are some discrepancies in the MTTF from the two models. The 95% CI is in general wide for all cases, which is due to extrapolation.

Table 5. Log-likelihood and AIC values of parametric and semiparametric models for the ADDT data from the three applications.

	Parametric models			Semiparametric models		
Applications	Loglik	df	AIC	Loglik	edf	AIC
Adhesive bond B	34.966	4	−61.933	38.726	5	−67.441
Seal strength	194.990	5	−379.981	199.745	6	−387.490
Adhesive formulation K	158.950	4	−309.901	163.989	8	−311.979

Table 6. Estimated MTTF and the associated 95% quantile-based CI at normal use condition, based on parametric and semiparametric models for the three applications. The failure threshold is set to be 70% and the time is in weeks (In the table, "est." means "estimate," "low." means "lower," and "upp." means "upper").

		Parametric			Semiparametric		
			95% CI			95% CI	
Applications	Normal use condition	est.	low.	upp.	est.	low.	upp.
Adhesive bond B	30°C	270	136	554	305	145	721
Seal strength	100°C	222	98	674	126	65	956
Adhesive formulation K	30°C	68	55	88	85	65	131

5.3 Model Assumption Checking

We conducted several graphical checks on the model assumptions for the three applications. To check the fitting of the mean structures, the fitted degradation paths for the parametric and semiparametric models are presented in Figures 7–9. All three figures show that the semiparametric models provide a good fit to the mean structure of the data. We can see that the proposed model is flexible in fitting ADDT data from different applications.

For each application, we also examined the Q-Q plot of standardized residuals and the pattern of standardized residuals versus fitted values. The Q-Q plot can reveal if the normality assumption holds well. The residuals can show if the constant variance assumption holds and if the mean structure (the semiparametric component for the mean function) describes the data well. Supplementary Figures S1 to S3 show the residual analyses for the adhesive bond B data, seal strength data, and adhesive formulation K data, respectively. Overall the plots show that the model assumptions hold well for these three applications.

5.4 Illustration of Quantile Function Estimation

For each application, the quantile functions and corresponding CI can be calculated. For illustrations, we use the adhesive bond B data as an example. Figure 10 shows the quantiles, t_α, and the 95% pointwise quantile-based bootstrap CI for four temperature

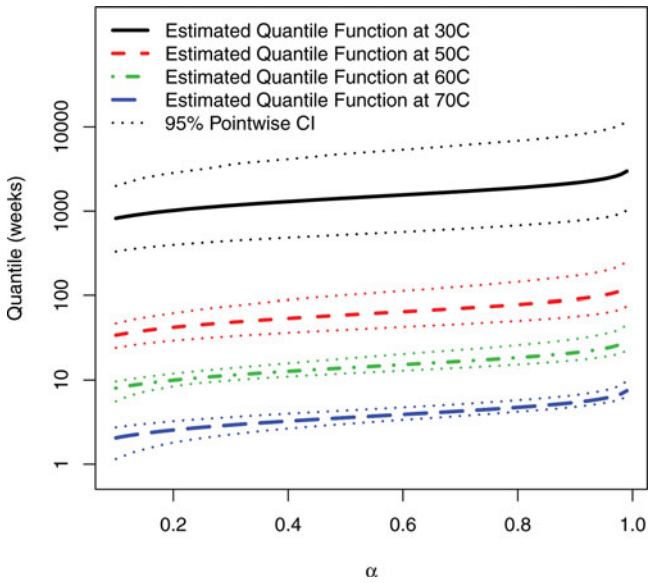

Figure 10. Estimates and CI of quantile functions at different temperature levels for adhesive bond B data.

levels for a range of α values. The dotted lines are the pointwise CI. Since the proposed method can allow users to set the particular failure threshold, in this illustration, we used the 40% failure threshold for the adhesive bond B data. The temperature for use condition is set to be 30°C. Note that the estimated quantile functions for different temperature levels in Figure 10 are parallel to each other (the y-axis is on log scale). This is because the α quantile for temperature level x_i is the α quantile at the baseline degradation level multiplied by the factor $\exp(\beta x_i)$.

6. Concluding Remarks and Areas for Future Work

In this article, we describe a new semiparametric degradation model for ADDT data based on monotonic B-splines. We develop estimation and inference procedures for the proposed model as well as methods for selecting knot locations for the B-splines. Our simulation results indicate that the proposed estimation procedures for the proposed semiparametric model perform well. Compared to parametric models, the semiparametric approach is more flexible, can be applied to a wide range of applications, and may be best suited as a generic method for ADDT data analysis for industrial standards. In addition, the semiparametric model is more robust to model misspecification than a parametric model approach. The proposed method is implemented in an R package named "ADDT" (Hong et al. 2016). Jin et al. (2017) provided illustrations on the use of the R package.

In the proposed method, we did not use equally spaced interior knots. The number and location of interior knots were determined using the AIC criterion. Due to the monotonicity constraints, the model fitting results are less sensitive to the number and locations of knots. This behavior is also observed in, for example, Meyer (2008), and Hong et al. (2015). The simulation study and applications demonstrated that the model chosen by AIC can provide an adequate fit to the data.

One possible application of the proposed semiparametric model could be for test planning. A test plan based on this model would be general enough for application to a variety of materials and also allow for testing of different models. The proposed model can serve a starting ground from which to test models against the data gathered rather than having to assume a given model prior to data collection. This would certainly serve as an interesting topic for future research.

The models considered here were solely scale-acceleration models. However, for certain types of products, a model with both scale and shape acceleration may describe the degradation path more appropriately. In this case, the scale-acceleration model may not be able to fit the data well resulting in poor predictions. Tsai et al. (2013) considered a parametric model with both scale and shape acceleration in test planning. Estimation and inference procedures for the semiparametric model would certainly be more complex with the introduction of a shape-acceleration parameter. It would be of great interest to pursue this in future research.

Although the focus of this article is on ADDT data, whether the proposed ADDT method can be used for RMDT is an interesting question for future research. For RMDT data, due to within unit correlations, one or more random effects are often used and this can introduce another layer of difficulty in the parameter estimation, which needs to be overcome in the future research.

Supplementary Materials

The following supplementary materials are available online.

Additional results: Additional results on residual analyses (pdf file).

Acknowledgments

The authors thank the editor, an associate editor, and three referees, for their valuable comments that helped us to improve this article. The authors acknowledge Advanced Research Computing at Virginia Tech for providing computational resources. The work by Hong was partially supported by the National Science Foundation under Grant CMMI-1634867 to Virginia Tech. The work by Yang was partially supported by the National Science Foundation under Grant CMMI-1404276 to Wayne State University.

References

Bollaerts, K., Eilers, P. H., and Mechelen, I. (2006), "Simple and Multiple P-Splines Regression with Shape Constraints," *British Journal of Mathematical and Statistical Psychology*, 59, 451–469. [2]

Carpenter, J. R., Goldstein, H., and Rasbash, J. (2003), "A Novel Bootstrap Procedure for Assessing the Relationship between Class Size and Achievement," *Applied Statistics*, 52, 431–443. [5]

De Boor, C. (2001), *A Practical Guide to Splines*, New York: Springer-Verlag. [4]

Efron, B., and Tibshirani, R. (1993), *An Introduction to the Bootstrap*, Boca Raton FL: Chapman and Hall/CRC. [6]

Eilers, P. H., and Marx, B. D. (1996), "Flexible Smoothing with B-splines and Penalties," *Statistical Science*, 11, 89–102. [2]

Escobar, L. A., Meeker, W. Q., Kugler, D. L., and Kramer, L. L. (2003), "Accelerated Destructive Degradation Tests: Data, Models, and Analysis," in *Mathematical and Statistical Methods in Reliability*, eds. B. H. Lindqvist and K. A. Doksum, River Edge, NJ: World Scientific Publishing Company, pp. 319–337. [1,2,9]

Fengler, M. R., and Hin, L.-Y. (2014), "A Simple and General Approach to Fitting the Discount Curve Under No-Arbitrage Constraints," available at *http://ssrn.com/abstract=2478719* [2]

Fritsch, F. N., and Carlson, R. E. (1980), "Monotone Piecewise Cubic Interpolation," *SIAM Journal on Numerical Analysis*, 17, 238–246. [4]

Goldfarb, D., and Idnani, A. (1983), "A Numerically Stable Dual Method for Solving Strictly Convex Quadratic Programs," *Mathematical Programming*, 27, 1–33. [4]

Gorjian, N., Ma, L., Mittinty, M., Yarlagadda, P., and Sun, Y. (2010), "A Review on Degradation Models in Reliability Analysis," in *Engineering Asset Lifecycle Management*, eds. D. Kiritsis, C. Emmanouilidis A. Koronios, and J. Mathew, New York: Springer, pp. 369–384. [2]

He, X., and Shi, P. (1998), "Monotone B-spline Smoothing," *Journal of the American Statistical Association*, 93, 643–650. [2,5]

Hofner, B., Kneib, T., and Hothorn, T. (2016), "A Unified Framework of Constrained Regression," *Statistics and Computing*, 26, 1–14. [2]

Hofner, B., Müller, J., and Hothorn, T. (2011), "Monotonicity-Constrained Species Distribution Models," *Ecology*, 92, 1895–1901. [2]

Hong, Y., Duan, Y., Meeker, W. Q., Stanley, D. L., and Gu, X. (2015), "Statistical Methods for Degradation Data with Dynamic Covariates Information and an Application to Outdoor Weathering Data," *Technometrics*, 57, 180–193. [2,12]

Hong, Y., Xie, Y., Jin, Z., and King, C. (2016), "ADDT: A Package for Analysis of Accelerated Destructive Degradation Test Data," R Package Version 1.1. Available at *https://cran.rproject.org*. [2,12]

Jin, Z., Xie, Y., Hong, Y., and Van Mullekom, J. H. (2017), "ADDT: An R package for Analysis of Accelerated Destructive Degradation Test Data," in *Statistical Modeling for Degradation Data*, eds. D. G. Chen, Y. L. Lio, H. K. T. Ng, and T. R. Tsai, NY: New York: Springer. [2,12]

Kanungo, T., Gay, D. M., and Haralick, R. M. (1995), "Constrained Monotone Regression of ROC Curves and Histograms using Splines and Polynomials," in *Proceedings of International Conference on Image Processing* (Vol. 2), IEEE, pp. 292–295. [2]

Leitenstorfer, F., and Tutz, G. (2007), "Generalized Monotonic Regression Based on B-splines with an Application to Air Pollution Data," *Biostatistics*, 8, 654–673. [2]

Li, M., and Doganaksoy, N. (2014), "Batch Variability in Accelerated-Degradation Testing," *Journal of Quality Technology*, 46, 171–180. [1,2,9]

Lu, C. J., and Meeker, W. Q. (1993), "Using Degradation Measures to Estimate a Time-to-Failure Distribution," *Technometrics*, 34, 161–174. [2]

Meeker, W. Q., Escobar, L. A., and Lu, C. J. (1998), "Accelerated Degradation Tests: Modeling and Analysis," *Technometrics*, 40, 89–99. [2]

Meeker, W. Q., Hong, Y., and Escobar, L. A. (2011), "Degradation Models and Data Analyses," in *Encyclopedia of Statistical Sciences*, New York: Wiley. [2]

Meyer, M. C. (2008), "Inference Using Shape-Restricted Regression Splines," *The Annals of Applied Statistics*, 2, 1013–1033. [2,12]

——— (2012), "Constrained Penalized Splines," *Canadian Journal of Statistics*, 40, 190–206. [5]

——— (2013), "A Simple New Algorithm for Quadratic Programming with Applications in Statistics," *Communications in Statistics—Simulation and Computation*, 42, 1126–1139. [4]

Nelson, W. B. (1990), *Accelerated Testing: Statistical Models, Test Plans, and Data Analysis*, New York: Wiley. [2]

Peng, C.-Y. (2016), "Inverse Gaussian Processes with Random Effects and Explanatory Variables for Degradation Data," *Technometrics*, 57, 100–111. [2]

Ramsay, J. O. (1988), "Monotone Regression Splines in Action," *Statistical Science*, 3, 425–441. [2]

Shiau, J. H., and Lin, H. (1999), "Analyzing Accelerated Degradation Data by Nonparametric Regression," *IEEE Transactions on Reliability*, 48, 149–158. [2]

Tsai, C.-C., Tseng, S.-T., Balakrishnan, N., and Lin, C.-T. (2013), "Optimal Design for Accelerated Destructive Degradation Tests," *Quality Technology and Quantitative Management*, 10, 263–276. [2,12]

UL746B (2013), *Polymeric Materials—Long Term Property Evaluations, UL 746B*, Northbrook, IL: Underwriters Laboratories, Incorporated. [2]

Vaca-Trigo, I., and Meeker, W. Q. (2009), "A Statistical Model for Linking Field and Laboratory Exposure Results for a Model Coating," in *Service Life Prediction of Polymeric Materials*, eds. J. Martin, R. A. Ryntz, J. Chin, and R. A. Dickie, New York: Springer: 29–43. [7]

Wang, H., Meyer, M. C., and Opsomer, J. D. (2013), "Constrained Spline Regression in the Presence of AR(p) Errors," *Journal of Nonparametric Statistics*, 25, 809–827. [5]

Wang, X., and Xu, D. (2010), "An Inverse Gaussian Process Model for Degradation Data," *Technometrics*, 52, 188–197. [2]

Xu, Z., Hong, Y., and Jin, R. (2016), "Nonlinear General Path Models for Degradation Data with Dynamic Covariates," *Applied Stochastic Models in Business and Industry*, 32, 153–167. [2]

Ye, Z., and Xie, M. (2015), "Stochastic Modelling and Analysis of Degradation for Highly Reliable Products," *Applied Stochastic Models in Business and Industry*, 31, 16–32. [2]

Ye, Z.-S., and Chen, N. (2014), "The Inverse Gaussian Process as a Degradation Model," *Technometrics*, 56, 302–311. [2]

Ye, Z.-S., Xie, M., Tang, L.-C., and Chen, N. (2014), "Semiparametric Estimation of Gamma Processes for Deteriorating Products," *Technometrics*, 56, 504–513. [2]

Zhou, R., Serban, N., and Gebraeel, N. (2014), "Degradation-Based Residual Life Prediction under Different Environments," *The Annals of Applied Statistics*, 8, 1671–1689. [2]